

SOLID-PHASE OXIDATION PROCESSES – HIGH TEMPERATURE OXIDATION RESISTANCE OF Ni-BASED ALLOYS

E. A. BASUKI^{a*}, F. PANGESTU^b, F. ADAM^c, A. A. KORDA^a, M. FADHLI^a,
D. PRAJITNO^d

^a*Department of Metallurgical Engineering, Faculty of Mining and Petroleum Engineering, Bandung Institute of Technology, 40 132 Bandung, Indonesia*

^b*PT. Tata Metal Lestari, Cikarang Selatan, 17 550 Bekasi, West Java, Indonesia*

^c*PT. Carsurin, Grogol, Petamburan, 11 470 Jakarta, Indonesia*

^d*Nuclear Technology Centre for Materials and Radiometry, National Atomic Agency of Indonesia, 40 132 Bandung, Indonesia*

E-mail: basuki@mining.itb.ac.id

ABSTRACT

Nickel-based superalloys are group of alloys dedicated for energy saving at high temperature applications. Oxidation has been considered as the most significant degradation mode of the alloy when they are used at high temperatures. Aluminum and chromium have been widely involved in the alloys to provide protective oxides of Al₂O₃ and Cr₂O₃ as they grow relatively slow. However, spallation of the protective scales might occur when the components experience thermal cyclic. Increasing the oxidation resistance of Ni-based alloys has been done by doping of yttrium and hafnium. However, investigations of the effect of germanium and zirconium on the oxidation behaviour of nickel-based alloys are quite few and the mechanisms have not been well explained. This study investigated the cyclic oxidation behaviour of Ge and Zr additions on Ni–9.6Cr–5.6Al–2.4Ti alloy at 900, 1000 and 1100°C. It was found that while Zr improved the cyclic oxidation resistance of the alloy it gave higher oxidation rates. Meanwhile, Ge addition improved the oxidation resistance of the alloys by decreasing the oxidation rate as well as improving the spalling resistance.

Keywords: nickel-based superalloys, cyclic oxidation, high temperature oxidation, effect of Ge and Zr.

* For correspondence.

AIMS AND BACKGROUND

Components used at high temperatures, such as those found in boiler as well as gas turbine engines, require materials with combination of mechanical properties and surface stability at relatively high temperatures¹. Development of high temperature alloys is mostly driven by the requirement to increase energy efficiency of such engines. Ni-based superalloy is a group of materials that are designed to have good fracture toughness, creep and fatigue properties, and resistance to high-temperature oxidation and hot corrosion^{2,3}. The development of Ni-based superalloys has been based primarily on the need to have alloys with high-temperature strength. The addition of relatively small amounts of Al and Ti in a binary Ni-Cr alloys increased the strength of the materials at high temperatures owing to the formation of coherent precipitates of the ordered intermetallic γ' -Ni₃(Al, Ti) (Ref. 4). This phase has unique mechanical properties in which the strength increases with temperature up to about 900°C. To provide materials with a high strength level at high temperatures, it has been found that the volume fraction of the γ' precipitates needs to be increased to a value of up to 70% (Ref. 5), and this is done by increasing the amount of Al and Ti in the alloys.

Cr, which is mostly dissolved in the γ -Ni matrix of nickel-based alloys, provides resistance to high-temperature oxidation and hot corrosion due to formation of a protective scale consisting relatively slow-growing oxide of Cr₂O₃ (Refs 6 and 7). The addition of Al in the alloys can also improve high-temperature oxidation resistance, since this element forms other protective scale of Al₂O₃, which is thermodynamically more stable than Cr₂O₃ (Ref. 8). However, the primary reason for the addition of Al in nickel alloys is to provide strength. Moreover, the maximum chemical content of Al necessary to optimise strength in these alloys is considered too low to produce the protective scale, Al₂O₃.

In high temperature applications involving cyclic stresses, the scales might easily crack and spall, resulting in shifting of the kinetic types of oxidation from parabolic type of oxidation behaviour to linear type indicating higher rate of oxidation. To improve the spalling resistance during cyclic oxidation of Ni-based superalloys, elements such as Y, Hf, Ce and Zr have been involved in relatively few amounts and the mechanisms of adherence of the oxides on the alloy surface has been proposed⁹⁻¹¹. Slight amount addition of Zr increased the adherence of Al₂O₃ and improves the oxidation resistance of the alloy¹². Nevertheless, relatively large amount of Zr eliminate the protective effect of alumina and consequently reduce the oxidation resistance. Addition of Zr up to 0.9 wt.% in iron aluminide alloys improved the oxidation behaviour of the alloy¹².

Ge has been employed in Si-Ge alloy that intensively used as semiconductor in electronic devices¹³. Oxidation behaviour in this system has been investigated and it is normally accepted that germanium increases the oxidation rate in this system. For example, silicon-germanium alloys with 28 and 36% of Ge oxidised at 700°C showed that mixed of GeO₂ and SiO₂ in the scales formed with the higher rate in higher Ge

content¹³. However, there have been reported that addition of Ge, in relatively small amount, in some alloy systems could reduce the oxidation rate and therefore improve oxidation resistance of the alloys^{14,15}. Addition of small amount Ge in silicide coatings improved isothermal and cyclic oxidation of Ti alloys through retarding the cracking and spalling of protective oxides¹⁴. Moreover, it was also found that addition of Ge decreased the oxidation resistance of near- α Ti alloy due to the formation of Ge rich layer on the interface of substrate-oxide layer¹⁴. The formation of Ge rich layer was believed due to the low solubility of Ge in TiO₂. Increasing the oxidation resistance obtained by small amount addition of Ge has also been found in the NiTi alloys oxidised at 800, 900 and 1000°C. In this study it was revealed that the highest oxidation resistance was found in alloys with 1.5% Ge addition¹⁵. In Pb free Sn – 0.7Cu solder, trace element of Ge was also reported improved the oxidation resistance of the alloy¹⁶. Furthermore, other study reported that in a nuclear reactor fuel cladding material of Zr–Nb–Mo–Ge alloy, the addition of Ge was found can increase the oxidation resistance of the material¹⁷. In Cr-based high temperature alloys of Cr–Cr₃Si system, addition of up to 2% Ge element has showed affect the spalling resistance of the scales at 1350°C (Ref. 18).

Among the rare elements, the effect of small amount addition of Ge on the oxidation behaviour of Ni-based superalloys has not been studied. This paper reports the investigations results on the effect of Ge and Zr addition on the cyclic oxidation behaviour of Ni–9.6Cr–5.6Al–2.4Ti model alloy at temperatures 900, 1000 and 1100°C. These results provide scientific consideration when Zr and Ge are involved to in nickel-based superalloys to improve the oxidation resistance at high temperature applications, such as in turbine blades of land based as well as aircraft gas turbine engines.

EXPERIMENTAL

Three Ni–9.6Cr–5.6Al–2.4Ti model alloys with nominal chemical compositions shown in Table 1 were melted in a single-arc furnace purged with high purity argon using pure element materials obtained from Sigma Aldrich. Prior to melting, the furnace chamber was purged with argon for 20 min and kept flowing during the melting. To ensure homogeneity, each alloy was melted four times. The alloy buttons were then homogenised at 1150°C for 100 h in a tube furnace in which argon was introduced to avoid from oxidation. After quenching in water, the alloys were then aged at 750°C for 2 h followed by air cooling. The as-aged model alloy buttons were sectioned to obtain 2.0 mm thick coupons with a single-side surface area of approximately 6 × 8 mm². Prior to the cyclic oxidation tests, the samples were ground to a 1200-grit finish using silicon carbide papers, and then ultrasonically cleaned in acetone followed by weighing of the clean samples. Polished samples of 1 µm finish were etched using chromic acid solution containing 50 ml H₂O, 150 ml HCl and 25 g CrO₃ for 10 s.

The microstructures of the model alloys were then observed under scanning electron microscope (SEM).

Table 1. Chemical composition of the alloys

Elements	Chemical composition (wt.%)			
	alloy 1	alloy 2	alloy 3	alloy 4
Ni	82.35	81.35	81.35	80.35
Al	5.60	5.60	5.60	5.60
Cr	9.60	9.60	9.60	9.60
Ti	2.40	2.40	2.40	2.40
C	0.05	0.05	0.05	0.05
Zr	0	1	0	1
Ge	0	0	1	1

Cyclic oxidation tests were conducted by heating the samples in a vertical tube furnace at three different temperatures of 900, 1000 and 1100°C up to 20 cycles. Each cycle represents heating the samples for 50 h followed by cooling to room temperature for 30 min. The weight change for each sample at each cycle was measured and plotted in curves of $\Delta W/A_0$ versus cycle number, where ΔW and A_0 , respectively, represent weight change and original total surface area of each sample. X-ray diffraction (XRD) analysis was used to identify the oxides existed on the samples after experienced 20 cycles of oxidation tests. The microstructures of the oxidised samples were observed under a scanning electron microscope (SEM), in which an energy dispersive spectroscopy (EDX) facility was attached. Chemical mappings were conducted to distinguish the elemental distribution in the scales.

RESULTS AND DISCUSSION

It was found that all model alloys had the same microstructures, as addition of either Zr or Ge of only 1% is predicted did not affect the microstructures of different model alloys. Figure 1 shows the microstructure of typically model alloys, consisting of γ -solid solution matrix and ordered intermetallic coherent precipitate of γ' -Ni₃ (Al, Ti). Two types of γ' , namely primary γ' and secondary γ' were found in all model alloys. This microstructure is essentially similar with that normally obtained in commercial nickel-based superalloys. However, no carbides were found in these model alloys as no carbon was added in the model alloys. The size of primary γ' was always larger than that of secondary γ' as the primary γ' formed at higher temperatures that provide higher activation energy for elements to diffuse much faster during nucleation and growth of the primary γ' .

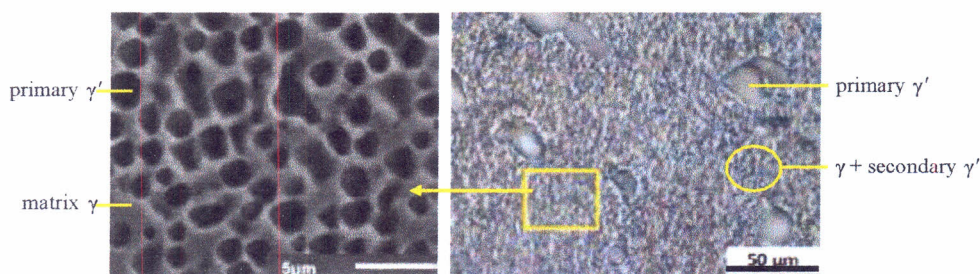


Fig. 1. Scanning and optical micrographs of typical microstructures of the model alloys

Figures 2, 3 and 4 provide the data of weight change during oxidation of model alloys for cycles up to 20 cycles at different temperatures. It is seen that most weight change is positive, indicating the dominance of oxide growth if compared with spalling of the scale. The characterisation results of the scales left on the surface of the samples after cyclic oxidation test for 20 cycles at 1100°C using XRD analysis, depicted in Figs 5–8, show various oxides. As higher temperature application is usually concerned, only XRD spectra of the sample oxidised at 1100°C are presented in the paper. Protective oxide of Al_2O_3 is mostly observed. However, unprotective TiO_2 occurred in addition of Cr_2O_3 and spinels NiCr_2O_4 .

Mappings of elements on the cross-sections of samples have been conducted to identify the distribution of oxides in the scales as well as in sub-scales. Most attention is addressed on samples of alloys 2, 3 and 4 after oxidised cyclically at 1100°C, where Ge and Zr are involved. The X-ray mapping results of these three alloys were depicted in Figs 9, 10 and 11, respectively. It is seen that in alloy 2, the outer part of the scale consists spinel of NiCr_2O_4 , TiO_2 located underneath of this spinel, while Al_2O_3 found on the interface between scale and substrate as well as distributed as particles in the outer part of the scale. Zirconium was preferably distributed as ZrO_2 along the grain boundary of substrate that connected with the scale. Nevertheless, some particles of ZrO_2 were also found distributed in outer part of the scale.

In alloy model 3, the outer part of the scale is dominated by TiO_2 , below which chromium oxide as Cr_2O_3 , was found as compact layer. However, Al_2O_3 mostly formed as internal oxides distributed underneath of the scale. Germanium was found distributed homogeneously in the scale as well as substrate. In alloy model 4, where Ge and Zr were added, the outer part of the scale was dominated by Cr_2O_3 and NiCr_2O_4 . A layer consisting of Al_2O_3 and TiO_2 found underneath of this Cr rich scale. Similar with that occurred in alloy model 3, Ge distributed homogeneously in the scale and substrate. However, higher distribution of Zr was found in the scale indicated the formation of Zr_2O_3 in the scale.

Oxidation of all model alloys resulted in the weight change due to two main contributions, i.e. pick-up of oxygen during oxidation which give weight gain, and oxide spalling which give weight loss. In total, the weight change (ΔW) in mg represents the different between sample weight after certain cycle and original weight of the sample

before oxidation was performed. Meanwhile, A_0 is the surface area of the original sample measured in cm^2 . Figures 2–4 show the relation between cycle number and $\Delta W/A_0$ at three different temperatures for 4 model alloys. Negative values of $\Delta W/A_0$ indicate loss of protective scale due to spallation.

As shown in Fig. 2, at 900°C , only Zr-modified alloy that had no negative values. All three non-modified, Ge and Ge + Zr modified alloys had negative values of $\Delta W/A_0$ at relatively early cycles up to 6 cycles. At 1000°C , however, the non-modified alloy experienced spallation of its protective scale at early cycles of up to 6 cycles followed by build-up the scale, even though continued spallation occurred at cycle 10. The other alloys principally had higher spalling resistance. Among these three alloys, Zr-modified alloys had higher weight gain and this indicates higher oxidation rate. At 1100°C , all alloys had positive weight gains. However, the Ge-modified alloys showed minimum weight gain and indicated slight spallation. Therefore, it is seen that at all temperatures the weight gain curves of alloy 2 always in highest position, and this indicates that the scale of alloy 2 has highest spallation resistance but it has highest oxidation rate. Addition of Ge in alloy 3 reduced the rate of oxidation as shown that the weight gain curve of alloy 3 is lower compared with that of alloy 1.

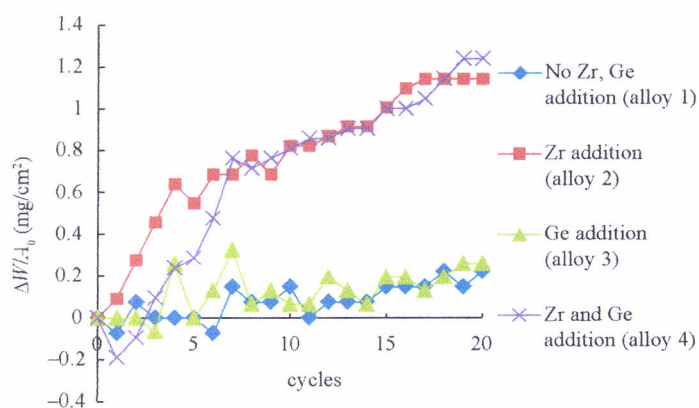


Fig. 2. Weight change of different alloy samples oxidised at 900°C for 20 cycles

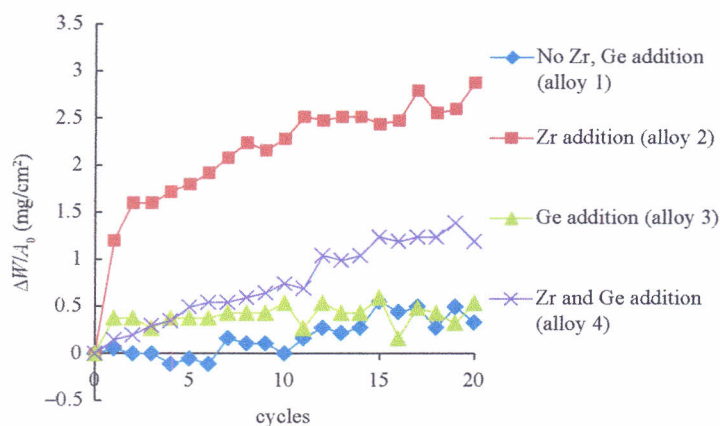


Fig. 3. Weight change of different alloy samples oxidised at 1000 °C for 20 cycles

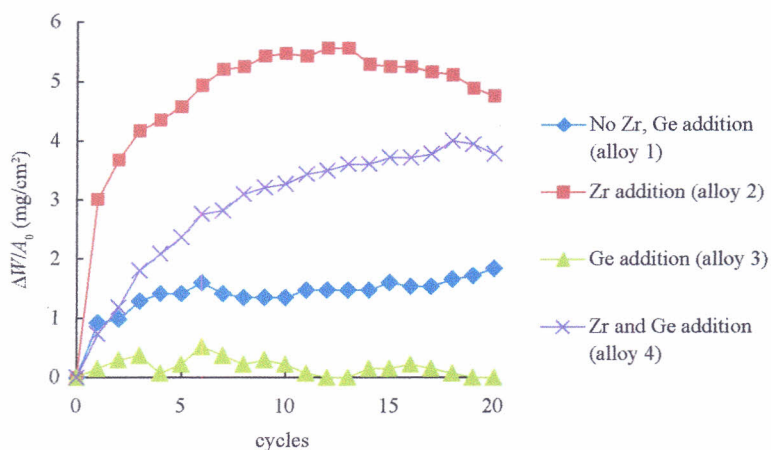


Fig. 4. Weight change of different alloy samples oxidised at 1100°C for 20 cycles

In this paper only XRD results of highest oxidation temperature, i.e. 1100°C, are presented, as shown in Figs 5–8. The scales of all four samples possessed different oxides. Alloy 1 had Al_2O_3 , NiAl_2O_4 and Cr_2O_3 , while alloy 2 contained Al_2O_3 , Cr_2O_3 , NiCr_2O_4 and NiO . Moreover, alloy 3 produced Al_2O_3 , NiAl_2O_4 , Cr_2O_3 and NiCr_2O_4 , while alloy 4 consisted Al_2O_3 , NiAl_2O_4 , Cr_2O_3 , NiCr_2O_4 , TiO_2 , NiO and ZrO_2 . The XRD patterns confirm the occurrence of Al_2O_3 at the surface of the scales of all samples. However, two types of spinels NiAl_2O_4 and NiCr_2O_4 were observed as the results of reactions between NiO and Al_2O_3 , and NiO and Cr_2O_3 , respectively. Meanwhile, NiO has reacted with Cr_2O_3 to form NiCr_2O_4 spinel.

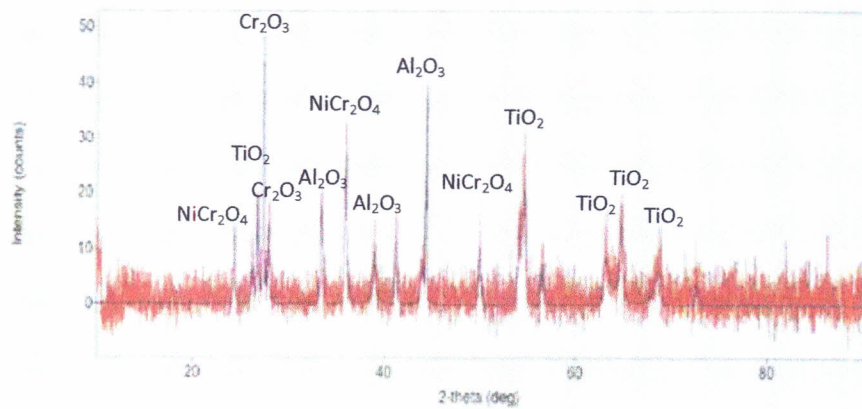


Fig. 5. Diffractogram of alloy 1 after heated cyclically at 1100 °C for 20 cycles

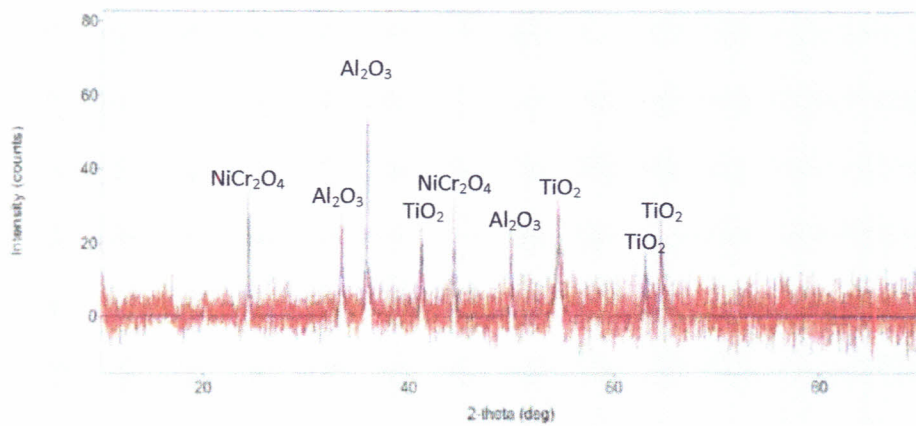


Fig. 6. Diffractogram of alloy 2 after heated cyclically at 1100 °C for 20 cycles

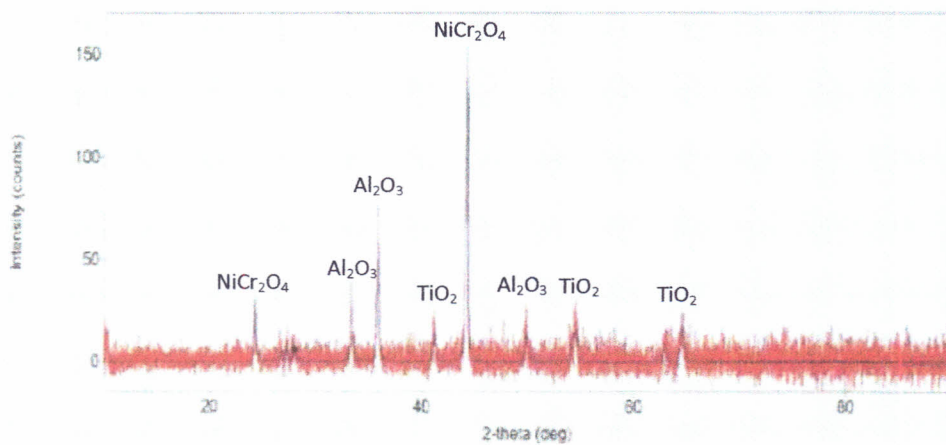


Fig. 7. Diffractogram of alloy 3 after heated cyclically at 1100 °C for 20 cycles

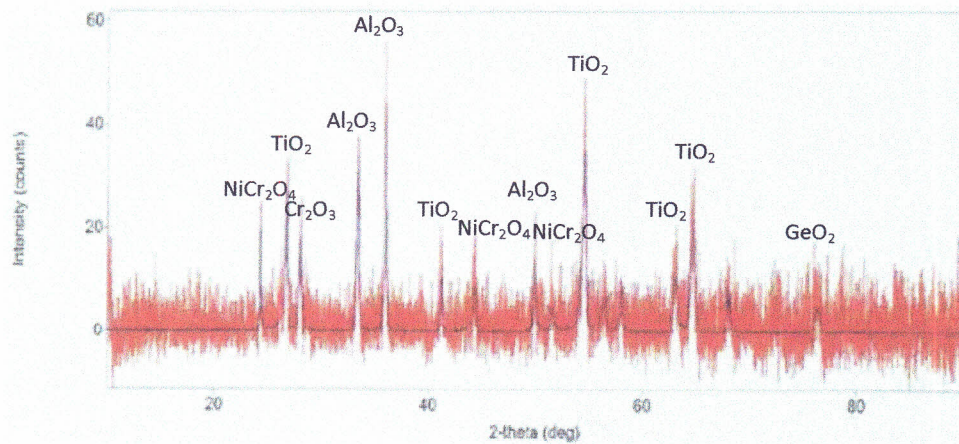


Fig. 8. Diffractogram of alloy 4 after heated cyclically at 1100 °C for 20 cycles

The X-ray mapping analysis was conducted to evaluate the distribution of elements in the cross section of the scales, from which distribution of oxides could be expected, as shown in Figs 9, 10 and 11. Only X-ray mapping of alloy 2, 3 and 4 are presented in this paper as these represents addition of Zr and Ge. X-ray mapping for alloy 2 containing Zr after cyclic oxidation at 1100°C for 20 cycles. As shown in Fig. 9, titanium oxide existed at the outer layer of the sample, but at relatively thin of about 5 μm . Chromium oxide, with relatively thick of about 20 μm , formed underneath of the titanium oxide layer. Aluminum oxide occurred as separate particles below chromium oxide layer as the result of internal oxidation.

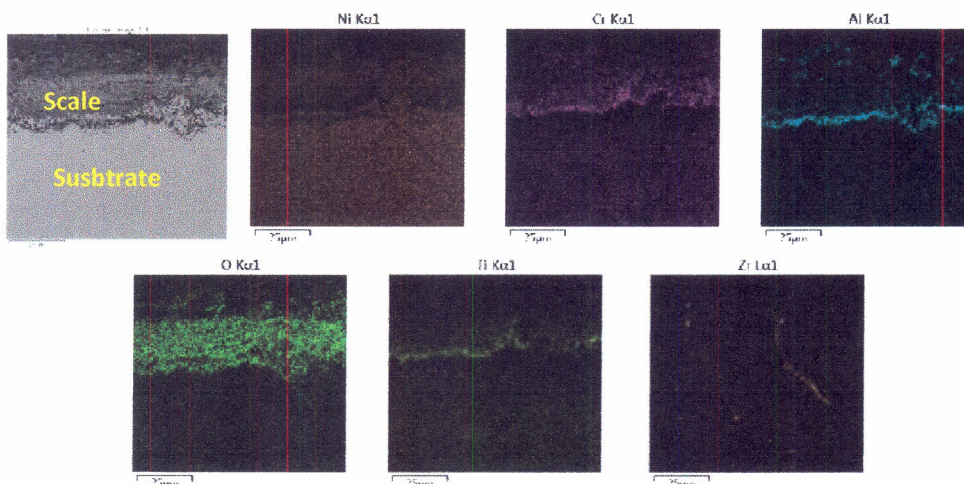


Fig. 9. X-rays mapping of model alloy 2 after cyclic oxidation at 1100°C for 20 cycles

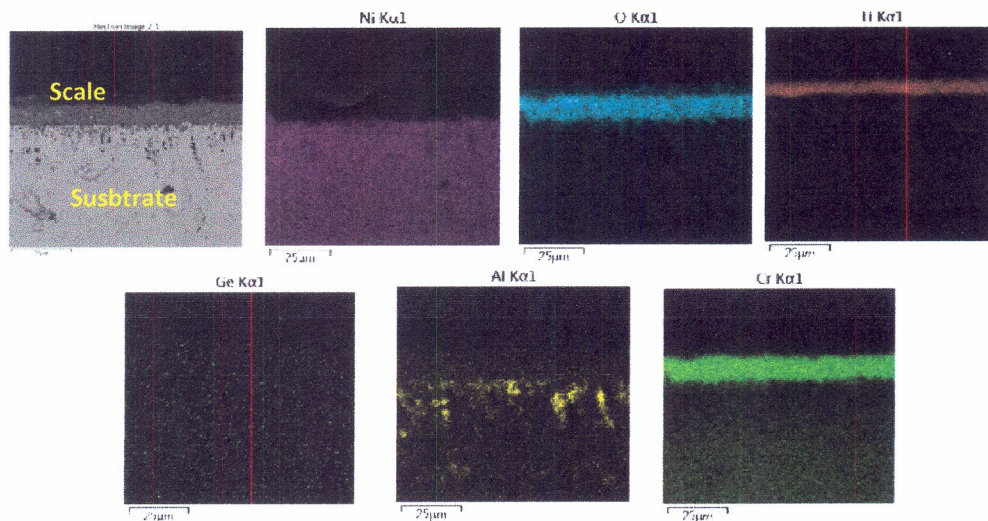


Fig. 10. X-rays mapping of model alloy 3 after cyclic oxidation at 1100°C for 20 cycles

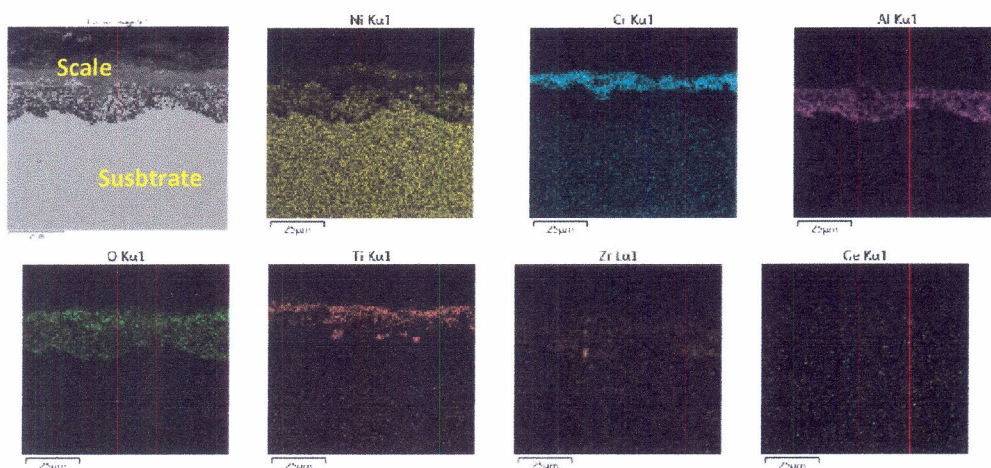


Fig. 11. X-rays mapping of model alloy 4 after cyclic oxidation at 1100°C for 20 cycles

Addition of Zr in model alloy 2 is believed to provide the driving force for formation of aluminium oxide underneath the spinel of NiCr_2O_4 . Figures 10 and 11 clearly show that different with that occur in model alloy 2, in model alloy 3 the Al_2O_3 formed as internal oxides. However, relatively compact Al_2O_3 layer developed at lower part of the scale. From the X-ray mapping it is seen that Zr distributed as ZrO_2 in several parts of the scale. Meanwhile, relatively homogeneous distribution of Ge, expected as GeO_2 , was found in alloys 2 and 4.

The X-ray mapping on alloy 4 after cyclic oxidation at 1100°C for 20 cycles, depicted in Fig. 11, shows that chromium oxide formed at the outer part of the scale,

while mixture of aluminium and titanium oxides occurred below the chromium oxides layer. However, germanium oxide was detected by XRD on the sample of alloy 3 and was not detected in sample of alloy 4. Thermodynamically, GeO_2 should be formed at 1100°C . However, in the Ellingham-Richardson diagram the position of GeO_2 formation line is slightly above the line for Cr_2O_3 (Ref. 19). While germanium atoms were distributed relatively homogeneously in the scales, zirconium atoms concentrated in certain spots indicated larger particles of ZrO_2 compared with GeO_2 .

CONCLUSIONS

Cyclic oxidation of Ni-9.6Cr-5.6Al-2.4Ti model alloys at 900, 1000 and 1100°C have been conducted in atmospheric condition. The scales containing mostly NiCr_2O_4 , Al_2O_3 and TiO_2 in which ZrO_2 and GeO_2 dispersed inside of the scale. TiO_2 formed on the outer part of the scale, while Al_2O_3 formed underneath of the scale. The study showed that increasing the spalling resistance was obtained when 1% Zr was added. However, higher consumption of metals was found in the alloy containing Zr. It is concluded that alloys with addition of 1% Ge provided relatively better spalling resistance compared with that no Ge addition. However, further experiments are still needed with involvement of Ge and Zr in different chemical composition variations.

REFERENCES

1. T. M. POLLOCK: Nickel-based Superalloys for Advanced Turbine Engine: Chemistry, Microstructure, and Properties. *J Propul Power*, **22** (2), 361 (2006).
2. A. SATO, H. HARADA, A. C. YEH, K. KAWAGISHI, T. KOBAYASHI, Y. KOIZUMI, T. YOKOKAWA, J. X. ZHANG: A 5th Generation SC Superalloy with Balanced High Temperature Properties and Processability. In: Proceedings of 11th International Symposium Superalloys, Pennsylvania, 14–18 September, 2008.
3. C. T. SIMS, N. S. STOLOFF, W. C. HAGEL: Superalloys II. John Wiley and Sons, 1987.
4. M. J. DONACHIE Jr., S. J. DONACHIE: Superalloys: a Technical Guide. 2nd ed. ASM International, Materials Park Ohio, 2002.
5. H. HARADA: Ni-base Superalloys and New Materials: Present Status and Possibilities in Future. *Journal Gas Turbine Society of Japan*, **28**, 278 (2008).
6. C. S. GIGGINS, F. S. PETTIT: Oxidation of Ni-Cr-Al between 1000°C and 1200°C . *J Electrochem Soc*, 1782 (1971).
7. K. KAWAGISHI, A. C. YEH, T. YOKOHAMA, T. KOBAYASHI, Y. KOIZUMI, H. HARADA: Development of an Oxidation-resistance High-strength Sixth-generation Single Crystal Superalloy. In: Proceedings of the International Symposium on Superalloys, TMS-238, Superalloys, Pennsylvania, 9–13 September, 2012, p. 189.
8. K. KAWAGISHI, A. SATO, T. KOBAYASHI, H. HARADA: Effect of Alloying Elements on the Oxidation Resistance of 4th Generation Ni-base Single Crystal Superalloys. *Journal of Japan Institute of Metals*, **69**, 249 (2005).
9. R. J. CHRISTENSEN, V. K. TOLPYGO, D. R. CLARKE: The Influence of the Reactive Element Yttrium on the Stress in Alumina Scales Formed by Oxidation. *Acta Mater*, **45**, 1761 (1997).
10. J. L. SMIALEK: Maintaining Adhesion of Protective Al_2O_3 Scales. *Journal of Metals*, **52**, 22 (2000).
11. S. XIU, W. LEI, L. YANG: Effects of Temperature and Rare Earth Content on Oxidation Resistance of Ni-based Superalloys. *Prog Nat Sci Mater Int*, **21**, 227 (2011).

12. Y. L. TSAI, S. F. WANG, H. Y. BOR, Y. F. HSU: Effect of Zr Addition on the Microstructure and Mechanical Behaviour of a Fine-grained Nickel Based Superalloy at Elevated Temperatures. *Mater Sci Eng A*, **607**, 294 (2014).
13. W. S. LIU, J. S. CHEN, M. A. NICHOLET: Instability of a GeSi_{1-x}O₂ Film on a GeSi_{1-x} Layer. *J Appl Phys*, **72**, 4015 (1992).
14. T. KITASHIMA, Y. YAMABE-MITARAI: Oxidation Behaviour of Germanium-and/or Silicon-bearing near α Titanium Alloys in Air. *Metall Mater Trans A*, **46A**, 2758 (2015).
15. F. S. HAMEED, A. H. HALEEM: Investigation the Effects of Germanium Addition on the Oxidation Behaviour of NiTi Shape Memory Alloy in Air. *Adv Nat Appl Sci*, **31**, (2017).
16. Q. WANG, G. GAN, Y. DU, D. YANG, G. MENG, H. WANG, Y. WU: Effect of Trace Ge on Wettability and High-temperature Oxidation Resistance of Sn–0.7Cu Lead-free Solder. *Mater Trans*, **57** (10), 1685 (2016).
17. B. BADRIYANA, M. NEVINGGO, A. KHALID, A. DIMYATI: Effect of β -Quenching on Oxidation Resistance of Zirconium Alloy ZrNbMoGe for Fuel Cladding Material. In: *Proceedings of the ICoNETS Conference, International Conference on Nuclear Energy Technology and Sciences*, San Diego, 2010, 2015.
18. A. DORCHEH-SOLEIMANI, W. DONNER, M. C. GALETZ: On Ultra-high Temperature Oxidation of Cr–Cr₃Si Alloys: Effect of Germanium. *Materials and Corrosion*, **65** (12), 1143 (2014).
19. N. A. TABET, M. A. SALIM: KRXPS Study of the Oxidation of Ge (001) Surface. *Appl Surf Sci*, **134** (1), 275 (1998).

Received 31 October 2018

Revised 6 November 2018

OXIDATION COMMUNICATIONS is the only scientific journal which, in its new form, is devoted to the global oxy-reduction interactions proceeding in nature.

OXIDATION COMMUNICATIONS acts as an international focus for modern fundamental and technological research in this rapidly developing field of science of exclusive importance for life.

The main topics and examples of specific areas of interest to the Journal are:

- a) gas-, liquid-, and solid-phase oxidation processes;
- b) the mechanism of action of inhibitors during the stabilisation of fuels, lubricating oils and greases, polymer materials and foodstuffs;
- c) oxidation reactions in the presence of homogeneous, heterogeneous, immobilised and enzymic catalytic systems;
- d) regulators of selective oxidation synthesis of valuable oxygen-containing compounds;
- e) biological and biochemical oxidation processes;
- f) photochemical oxy-reduction interactions;
- g) methods for prognosis and evaluation of performance terms or/and storage terms of the materials, as mentioned above in b);
- h) tribochemical interactions on metal and other surfaces in the presence of molecular oxygen or its activated species;
- i) methods for solar and chemical energy accumulation;
- j) studies on the nature of intermediates, generated in the course of oxidation;
- k) technological aspects of oxidation processes of special interest to the petrochemistry, pharmaceuticals, food and agrochemical industries;
- l) ecologically friendly oxidative processes for the atmosphere, soils and water.

The term 'oxidation' is interpreted widely, including both organic and inorganic compounds as oxidising agents during the oxidation

processes of organic and inorganic substrates. The interdisciplinary nature of the Journal ensures appeal to direct exchange

of ideas and contributions among academic and industrial scientists. The Journal is publishing refereed authoritative review articles,

papers covering original studies and also short communications, including preliminary results of a particular interest.

Designed to: chemists, researchers in the field of physical chemistry, petrochemistry, organic synthesis, catalysis, molecular biology and

biochemistry, tribochemistry, polymer and engineering chemistry.

The Journal is covered and evaluated in Elsevier products - Reaxys and Scopus, SJR - SCImago Journal & Country Rank. The Journal is included in EBSCOhost: Academic Search Complete, Academic Search Ultimate, The Belt and Road Initiative Reference Source. The Journal is refereed in Chemical Abstract Services.

OXIDATION COMMUNICATIONS

ISSN 0209-4541

Year 2018

Book 4

CONTENTS

Gas-phase oxidation processes

Z. NIKOLAEVA. Modelling of Ground Level Ozone Concentration in the Atmosphere459

E. A. BASUKI, F. PANGESTU, F. ADAM, A. A. KORDA, M. FADHLI, D. PRAJITNO. Solid-phase Oxidation Processes – High Temperature Oxidation Resistance of Ni-based Alloys.....465

Theoretical investigation of selective oxidation synthesis

V. A. BABKIN, G. A. SAVIN, V. YU. DMITRIEV, A. V. IGNATOV et al. Quantum Chemical Investigation of the Acylation Reaction of Bicyclophosphites by Acyl Galogenides.....477

Action of inhibitors and antimicrobial compounds

KH. QADER, K. ABDUL. Antioxidant Activity, Total Phenolic and Flavonoid Content of Broccoli (*Brassica oleracea* var. *Italica*) as Affected by Foliar Application.....483

A. ALINJ, B. SEITI, K. KHANARI, E. SKENDULI. Study on Protection Role of N (1 naphthyl)ethylenediamine Dihydrochloride Monomethanolate in the Corrosion of Carbon Steel in Hydrochloric Acid Environment.....494

KHALIL UR REHMAN, NAZISH JAHAN, MUHAMMAD ASIF HANIF. Antimicrobial Activity and GC-MS Characterisation of Essential Oil of Milk Thistle.....501

Y. KOLEVA, S. GEORGIEVA. Prediction of the Probable Behaviour of Some Beta-lactam Antibiotics on Human Health and Environment.....507

Biological and biochemical oxidation processes

B. MIDYUROVA, V. NENOV. Multidimensional Modelling of Cathode Design for Eventual Application in Bio-electrochemical Systems.....517

N. AGOVA, Y. KOLEVA, S. GEORGIEVA. Probable Metabolic Activity of Bexarotene in the Liver.....526

G. S. SIMONYAN, A. G. SIMONYAN, M. L. SAYADYAN, D. N. SARSEKOVA, G. P. PIRUMYAN. Analysis of Environmental Status of Wood and Shrub Vegetation by the Armenian Index of Environmental Quality.....533

Methods for composition investigation of biological products

L. DOSPATLIEV, V. LOZANOV, M. IVANOVA, P. PAPAHOV, P. SUGAREVA, Z. PETKOVA, D. BOJILOV. Comparison of Free Amino Acid Compositions of Stem and Cap in Wild Edible Mushrooms, Bulgaria.....542

Overall ecology

R. IOSSIFOV. Critical Swimming Speed – Intensity Level or Just a Statistical Parameter?.....550

Authors Index.....567

Founding Editor

D. GAL, Hungary

Editor-in-Chief

S. K. IVANOV, Bulgaria

Editors

M. I. BONEVA, Bulgaria

Zh. D. KALITCHIN, Bulgaria

Editorial Board

R. L. AUGUSTINE, USA

S. W. BENSON, USA

S. BOURBIGOT, France

D. BRADLEY, UK

A. M. BRAUN, Germany

E. B. BURLAKOVA, Russia

J. DAHLMANN, Germany

A. D'AMORE, Italy

S. DOBE, Hungary

Sh. GAO, China

N. GETOFF, Austria

V. K. GUPTA, India

J. HAPPEL, USA

J. A. HOWARD, Canada

M. F. R. MULCAHY, Australia

A. NEMETH, Hungary

E. NIKI, Japan

K. OHKUBO, Japan

R. A. SHELDON, The Netherlands

G. E. ZAIKOV, Russia

J. J. ZIOLKOWSKI, Poland

ZUWEI Xi, China